

---

# TRACT: Denoising Diffusion Models with Transitive Closure Time-Distillation

---

<b>David Berthelot*</b> Apple	<b>Arnaud Autef</b> Apple	<b>Jierui Lin</b> Apple	<b>Dian Ang Yap</b> Apple	<b>Shuangfei Zhai</b> Apple
<b>Siyuan Hu</b> Apple	<b>Daniel Zheng</b> Apple	<b>Walter Talbott</b> Apple	<b>Eric Gu</b> Apple	

## Abstract

Denoising Diffusion models have demonstrated their proficiency for generative sampling. However, generating good samples often requires many iterations. Consequently, techniques such as binary time-distillation (BTD) have been proposed to reduce the number of network calls for a fixed architecture. In this paper, we introduce TRAnsitive Closure Time-distillation (TRACT), a new method that extends BTD. For single step diffusion, TRACT improves FID by up to  $2.4\times$  on the same architecture, and achieves new single-step Denoising Diffusion Implicit Models (DDIM) state-of-the-art FID (7.4 for ImageNet64, 3.8 for CIFAR10). Finally we tease apart the method through extended ablations. The PyTorch [37] implementation will be released soon.

## 1 Introduction

Diffusion models [45, 47, 15] represent state-of-the-art generative models for many domains and applications. They work by learning to estimate the score of a given data distribution, which in practice can be implemented with a denoising autoencoder following a noise schedule. Training a diffusion model is arguably much simpler compared to many alternative generative modeling approaches, e.g., GANs [10], normalizing flows [7] and auto-regressive models [3]. The loss is well-defined and stable; there is a large degree of flexibility to design the architecture; and it directly works with continuous inputs without the need for discretization. These properties make diffusion models demonstrate excellent scalability to large models and datasets, as shown in recent works in diverse domains such as image generation [16, 6], image or audio super-resolution [27, 13, 28, 43], audio and music synthesis [31, 35, 25, 4, 36], language models [29, 9, 19, 2], and cross-domain applications such as text-to-image and text-to-speech [40, 42, 22, 39, 41]

Despite the empirical success, inference efficiency remains a major challenge for diffusion models. As shown in [48], the inference process of diffusion models can be cast as solving a neural ODE [5], where the sampling quality improves as the discretization error decreases. As a result, up to thousands of denoising steps are used in practice in order to achieve high sampling quality. This dependency on a large number of inference steps makes diffusion models less favorable compared to one-shot sampling methods, e.g., GANs, especially in resource-constrained deployment settings.

Existing efforts for speeding up inference of diffusion models can be categorized into three classes: (1) reducing the dimensionality of inputs [41, 50, 12]; (2) improving the ODE solver [24, 32]; and (3) progressively distilling the output of a teacher diffusion model to a student model with fewer steps [44, 34]. Among these, the progressive distillation approach is of special interest to us. It uses the fact that with a Denoising Diffusion Implicit Model (DDIM) inference schedule [46], there is a

---

\*correspondance to dberthelot@apple.com

deterministic mapping between the initial noise and the final generated result. This allows one to learn an efficient student model that approximates a given teacher model. A naive implementation of such distillation would be prohibitive, as for each student update, the teacher network needs to be called  $T$  times (where  $T$  is typically large) for each student network update. Salimans and Ho [44] bypass this issue by performing progressive binary time distillation (BTD). In BTD, the distillation is divided into  $\log_2(T)$  phases, and in each phase, the student model learns the inference result of two consecutive teacher model inference steps. Experimentally, BTD can reduce the inference steps to four with minor performance loss on CIFAR10 and 64x64 ImageNet.

In this paper, we aim to push the inference efficiency of diffusion models to the extreme: one-step inference with high quality samples. We first identify critical drawbacks of BTD that prevent it from achieving this goal: 1) objective degeneracy, where the approximation error accumulates from one distillation phase to the next, and 2) the prevention of using aggressive stochastic weights averaging (SWA) [21] to achieve good generalization, due to the fact that the training course is divided into  $\log_2(T)$  distinct phases.

Motivated by these observations, we propose a novel diffusion model distillation scheme named TRAnsitive Closure Time-Distillation (TRACT). In a nutshell, TRACT trains a student model to distill the output of a teacher model’s inference output from step  $t$  to  $t'$  with  $t' < t$ . The training target is computed by performing one step inference update of the teacher model to get  $t \rightarrow t - 1$ , followed by calling the student model to get  $t - 1 \rightarrow t'$ , in a bootstrapping fashion. At the end of distillation, one can perform one-step inference with the student model by setting  $t = T$  and  $t' = 0$ . We show that TRACT can be trained with only one or two phases, which avoids BTD’s objective degeneracy and incompatibility with SWA.

Experimentally, we verify that TRACT drastically improves upon the state-of-the-art results with one and two steps of inference. Notably, it achieves single-step FID scores of 7.4 and 3.8 for 64x64 ImageNet and CIFAR10 respectively.

## 2 Related Work

**Background** DDIMs [46] are a subclass of Denoising Diffusion Probabilistic Models (DDPM) [15] where the original noise is reused at every step  $t$  of the inference process. Typically DDIMs use a  $T$ -steps noise schedule  $\gamma_t \in [0, 1)$  for  $t \in \{1, \dots, T\}$ . By convention,  $t = 0$  denotes the noise-free step and therefore  $\gamma_0 = 1$ . In the variance preserving (VP) noisification setting, a noisy sample  $x_t$  is produced from the original sample  $x_0$  and some Gaussian noise  $\epsilon$  as follows:

$$x_t = x_0\sqrt{\gamma_t} + \epsilon\sqrt{1 - \gamma_t} \tag{1}$$

A neural network  $f_\theta$  is trained to predict either the signal, the noise or both. The estimations of  $x_0$  and  $\epsilon$  at step  $t$  are denoted as  $x_{0|t}$  and  $\epsilon_{|t}$ . For the sake of conciseness, we only detail the signal prediction case. During the denoisification phase, the predicted  $x_{0|t}$  is used to estimate  $\epsilon_{|t}$  by substitution in Equation (1):

$$x_{0|t} := f_\theta(x_t, t) \text{ and } \epsilon_{|t} = \frac{x_t - x_{0|t}\sqrt{\gamma_t}}{\sqrt{1 - \gamma_t}}$$

These estimates allow inference, by substitution in Equation (1), of  $x_{t'}$  for any  $t' \in \{0, \dots, T\}$ :

$$x_{t'} = \delta(f_\theta, x_t, t, t') := x_t \frac{\sqrt{1 - \gamma_{t'}}}{\sqrt{1 - \gamma_t}} + f_\theta(x_t, t) \frac{\sqrt{\gamma_{t'}(1 - \gamma_t)} - \sqrt{\gamma_t(1 - \gamma_{t'})}}{\sqrt{1 - \gamma_t}} \tag{2}$$

Here we introduced the step function  $\delta(f_\theta, x_t, t, t')$  to denote DDIM inference from  $x_t$  to  $x_{t'}$ .

**Advanced ODE solvers** A common framework in the denoisification process is to use stochastic differential equations (SDEs) that maintain the desired distribution  $p$  as the sample  $x$  evolves over time [24, 48]. Song et. al. presented a corresponding probability flow ordinary differential equation (ODE) with the initial generated noise as the only source of stochasticity. Compared to SDEs, ODEs can be solved with larger step sizes as there is no randomness between steps.

Another advantage of solving probability flow ODEs is that we can use existing numerical ODE solvers to accelerate sampling in the denoisification phase. However, solving ODEs numerically approximates the true solution trajectory due to the truncation error from the solver. Popular numerical

ODE solvers include first-order Euler’s method and higher-order methods such as Runge-Kutta (RK) [49]. Karras et. al. apply Heun’s 2<sup>nd</sup> order method [1] in the family of explicit second-order RK to maintain a tradeoff between truncation error and number of function evaluations (NFEs) [24, 23, 8].

However, existing ODE solvers are unable to generate high-quality samples in the few-step sampling regime (we loosely define few-steps regime in  $\approx 5$  steps). RK methods may suffer from numerical issues with large step sizes [18, 17]. Our work provides an orthogonal direction to these ODE solvers, and TRACT outputs can be further refined with higher-order methods.

**Diffusion model distillation** The idea of distilling a pretrained diffusion model to a single step student is first introduced in [33]. Despite encouraging results, it suffers from high training costs and sampling quality degradation. This idea is later extended in [44, 20, 34], where one progressively distills a teacher model to a student by reducing its total steps by a factor of two.

Specifically, in Binary Time-Distillation (BTD) [44], a student network  $g_\phi$  is trained to replace two denoising steps of the teacher  $f_\theta$ . Using the step function notation,  $g_\phi$  is modeled to hold this equality:

$$\delta(g_\phi, x_t, t, t-2) \approx x_{t-2} := \delta(f_\theta, \delta(f_\theta, x_t, t, t-1), t-1, t-2) \quad (3)$$

From this definition, we can determine the target  $\hat{x}$  that makes the equality hold (see Appendix A.1):

$$\hat{x} = \frac{x_{t-2}\sqrt{1-\gamma_t} - x_t\sqrt{1-\gamma_{t-2}}}{\sqrt{\gamma_{t-2}}\sqrt{1-\gamma_t} - \sqrt{\gamma_t}\sqrt{1-\gamma_{t-2}}} \quad (4)$$

The signal loss is inferred by rewriting the noise prediction error (see Appendix A.2), yielding:

$$\mathcal{L}(\phi) = \frac{\gamma_t}{1-\gamma_t} \|g_\phi(x_t, t) - \hat{x}\|_2^2 \quad (5)$$

Once a student has been trained to completion, it becomes the teacher and the process is repeated until the final model has the desired number of steps.  $\log_2 T$  training phases are required to distill a  $T$ -steps teacher to a single-step model and each trained student requires half the sampling steps of its teacher to generate high-quality samples.

### 3 Method

We propose TRANSITIVE Closure Time-Distillation (TRACT), an extension of BTD, that reduces the number of distillation phases from  $\log_2 T$  to a small constant, typically 1 or 2. We focus on the VP setting used in BTD first, but the method itself is independent of it and we illustrate it in the Variance Exploding (VE) setting at the end of the section. While TRACT also works for noise-predicting objectives, we demonstrate it on signal-prediction where the neural network predicts an estimate of  $x_0$ .

#### 3.1 Motivation

We conjecture that the final quality of samples from a distilled model is influenced by the number of distillation phases and the length of each phase. As later validated in the experiments section, we consider two potential explanations as to why it is the case.

##### Objective degeneracy

In BTD, the student in the previous distillation phase becomes the teacher for the next phase. The student from the previous phase has a positive loss which yields an imperfect teacher for the next phase. These imperfections accumulate over successive generations of students which leads to objective degeneracy.

##### Generalization

Stochastic Weight Averaging (SWA) has been used to improve the performance of neural networks trained for DDPMs [15]. With Exponential Moving Average (EMA), the momentum parameter is limited by the training length: high momentum yields high-quality results but leads to over-regularized models if the training length is too short. This ties in with the time-distillation problem since the total training length is directly proportional to the number of training phases.

### 3.2 TRACT

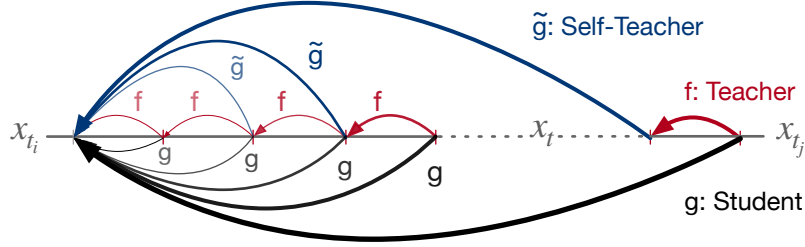


Figure 1: Transitive Closure Distillation of a group  $\{t_i, \dots, t_j\}$ .

TRACT is a multi-phase method where each phase distills  $T$ -steps schedule to  $T' < T$  steps, and is repeated until the desired number of steps is reached. In a phase, the  $T$ -steps schedule is partitioned into  $T'$  contiguous groups. The partitioning strategy is left open; for example, in our experiments we used equally-sized groups as demonstrated in Algorithm (1).

Our method can be seen as an extension of BTM which is not constrained by  $T' = T/2$ . However, computational implications arise from the relaxation of this constraint, such as the estimation of  $x_{t'}$  from  $x_t$  for  $t' < t$ .

For a contiguous segment  $\{t_i, \dots, t_j\}$ , we model the student  $g_\phi$  to jump to step  $t_i$  from any step  $t_i < t \leq t_j$  as illustrated in Figure (1):

$$\delta(g_\phi, x_t, t, t_i) = \delta(f_\theta, \delta(f_\theta, \dots \delta(f_\theta, x_t, t, t-1), \dots), t_{i+1}, t_i) \quad (6)$$

The student  $g$  is specified to encompass  $(t_j - t_i)$  denoising steps of  $f$ . However, this formulation could require multiple calls of  $f$  during training, leading to prohibitive computational costs.

To resolve this issue, we use a self-teacher whose weights are an exponential moving average (EMA) [21] of the student  $g$ . This approach is inspired from semi-supervised learning [26], reinforcement learning [30] and representation learning [11]. For a student network  $g$  with weights  $\phi$ , we denote the EMA of its weights as  $\tilde{\phi} = \text{EMA}(\phi, \mu_S)$  where  $\mu_S \in [0, 1]$ , the momentum, is an hyper-parameter.

The transitive closure operator can now be modeled with self-teaching by rewriting the closure in Equation (6) as a recurrence:

$$\delta(g_\phi, x_t, t, t_i) \approx x_{t_i} := \delta(g_{\tilde{\phi}}, \delta(f_\theta, x_t, t, t-1), t-1, t_i) \quad (7)$$

From this definition, we can determine the target  $\hat{x}$  that makes the equality hold using the same method as for Equation (4), see Appendix A.1 for details:

$$\hat{x} = \frac{x_{t_i} \sqrt{1 - \gamma_t} - x_t \sqrt{1 - \gamma_{t_i}}}{\sqrt{\gamma_{t_i}} \sqrt{1 - \gamma_t} - \sqrt{\gamma_t} \sqrt{1 - \gamma_{t_i}}} \quad (8)$$

For the special case  $t_i = t - 1$ , we have  $\hat{x} = f_\theta(x_t, t)$ .

The loss is the standard signal-predicting DDIM distillation training loss, e.g. for a target value  $\hat{x}$ :

$$\mathcal{L}(\phi) = \frac{\gamma_t}{1 - \gamma_t} \|g_\phi(x_t, t) - \hat{x}\|_2^2 \quad (9)$$

### 3.3 Adapting TRACT to a Runge-Kutta teacher and Variance Exploding noise schedule

To illustrate its generality, we apply TRACT to teachers from Elucidating the Design space of diffusion Models (EDM) [24] that use a VE noise schedule and an RK sampler.

**VE noise schedules** A VE noisification process is parameterized by a sequence of noise standard deviations  $\sigma_t \geq 0$  for  $t \in \{1, \dots, T\}$  with  $\sigma_1 = \sigma_{min} \leq \sigma_t \leq \sigma_T = \sigma_{max}$ , and  $t = 0$  denotes the noise-free step  $\sigma_0 = 0$ . A noisy sample  $x_t$  is produced from an original sample  $x_0$  and Gaussian noise  $\epsilon$  as follows:

$$x_t = x_0 + \sigma_t \epsilon \quad (10)$$

---

**Algorithm 1** Single-phase TRACT training from T timesteps to T/S timesteps for groups of size S.

---

```
1: Inputs Training data  $\mathcal{X}$ , time schedule  $\gamma \in \mathbb{R}^T$ ,  $f_\theta$  is the teacher,  $g_\phi$  is the student being trained
2:  $\phi \leftarrow \theta$ ;  $\tilde{\phi} \leftarrow \theta$  ▷ Initialize self-teacher and student from teacher
3: for batch of training data  $(x^{(b)}; b \in \{1, \dots, B\}) \sim \mathcal{X}$  do
4:    $\mathcal{L}(\phi) \leftarrow 0$ 
5:   for  $b = 1$  to  $B$  do
6:     sample  $\epsilon \sim \mathcal{N}(0, 1)$  ▷ Same shape as  $x^{(b)}$ 
7:     sample  $s \sim \{0, S, 2S, \dots, T - S\}$  ▷ Sample the group starting position
8:     sample  $p \sim \{1, \dots, S\}$  ▷ Sample the index within the group
9:      $t \leftarrow s + p$  ▷ Time step to distill
10:     $x_t \leftarrow x^{(b)} \sqrt{\gamma_t} + \epsilon \sqrt{1 - \gamma_t}$  ▷ Generate noisy sample
11:     $x_{t-1} \leftarrow (x_t \sqrt{1 - \gamma_{t-1}} + f_\theta(x_t, t) (\sqrt{\gamma_{t-1}(1 - \gamma_t)} - \sqrt{\gamma_t(1 - \gamma_{t-1})})) / \sqrt{1 - \gamma_t}$ 
12:    if  $s = t - 1$  then
13:       $x_s \leftarrow x_{t-1}$ 
14:    else
15:       $x_s \leftarrow (x_{t-1} \sqrt{1 - \gamma_s} + g_{\tilde{\phi}}(x_{t-1}, t-1) (\sqrt{\gamma_s(1 - \gamma_{t-1})} - \sqrt{\gamma_{t-1}(1 - \gamma_s)})) / \sqrt{1 - \gamma_{t-1}}$ 
16:    end if
17:    target  $\hat{x} \leftarrow (x_s \sqrt{1 - \gamma_t} - x_t \sqrt{1 - \gamma_s}) / (\sqrt{\gamma_s} \sqrt{1 - \gamma_t} - \sqrt{\gamma_t} \sqrt{1 - \gamma_s})$ 
18:     $\mathcal{L}(\phi) \leftarrow \mathcal{L}(\phi) + \max(1, \gamma_t / (1 - \gamma_t)) \frac{1}{B} \|g_\phi(x_t, t) - \text{stop\_gradient}(\hat{x})\|_2^2$ 
19:  end for
20:  Compute gradients of  $\mathcal{L}(\phi)$  and update parameters  $\phi$ 
21:  Update  $\tilde{\phi} \leftarrow \text{EMA}(\phi, \mu_S)$  ▷  $\mu_S$  is a hyper-parameter for EMA momentum
22: end for
```

---

**RK step function** Following on the EDM approach, we use an RK sampler for the teacher and distill it to a DDIM sampler for the student. The corresponding step functions are  $\delta_{RK}$  and  $\delta_{DDIM-VE}$ , respectively. The  $\delta_{RK}$  step function to estimate  $x_{t'}$  from  $x_t, t > 0$ , is defined as:

$$\delta_{RK}(f_\theta, x_t, t, t') := \begin{cases} x_t + (\sigma_{t'} - \sigma_t)\epsilon(x_t, t) & \text{if } t' = 0 \\ x_t + \frac{1}{2}(\sigma_{t'} - \sigma_t) [\epsilon(x_t, t) + \epsilon(x_t + (\sigma_{t'} - \sigma_t)\epsilon(x_t, t), t)] & \text{otherwise} \end{cases} \quad (11)$$

where  $\epsilon(x_t, t) := \frac{x_t - f_\theta(x_t, t)}{\sigma_t}$ .

The  $\delta_{DDIM-VE}$  step function to estimate  $x_{t'}$  from  $x_t, t > 0$ , is defined as:

$$\delta_{DDIM-VE}(f_\theta, x_t, t, t') := f_\theta(x_t, t) \left(1 - \frac{\sigma_{t'}}{\sigma_t}\right) + \frac{\sigma_{t'}}{\sigma_t} x_t \quad (12)$$

Then, learning the transitive closure operator via self-teaching requires:

$$\delta_{DDIM-VE}(g_\phi, x_t, t, t_i) \approx x_{t_i} := \delta_{DDIM-VE}(g_{\tilde{\phi}}, \delta_{RK}(f_\theta, x_t, t, t-1), t-1, t_i) \quad (13)$$

From this definition, we can again determine the target  $\hat{x}$  that makes the equality hold:

$$\hat{x} = \frac{\sigma_t x_{t_i} - \sigma_{t_i} x_t}{\sigma_t - \sigma_{t_i}} \quad (14)$$

The loss is then a weighted loss between the student network prediction and the target. We follow the weighting and network preconditioning strategies introduced in the EDM paper [24]:

$$\mathcal{L}(\phi) = \lambda(\sigma_t) \|g_\phi(x_t, t) - \hat{x}\|_2^2 \quad (15)$$

The resulting distillation algorithm and details on the derivation of  $\delta_{RK}$ ,  $\delta_{DDIM-VE}$  as well as the training target  $\hat{x}$  can be found in Appendix A.8.

## 4 Experiments

We present results with TRACT on two image generation benchmarks: CIFAR-10 and class-conditional 64x64 ImageNet. On each dataset, we measure the performance of our distilled models

Method	NFEs	FID	Parameters
TRACT-EDM-256M*	1	<b>3.78</b> $\pm$ 0.01	56M
DFNO [51] <sup>†</sup>		4.12	65.8M
TRACT-EDM-96M*		4.17 $\pm$ 0.03	56M
TRACT-256M		4.45 $\pm$ 0.05	60M
TRACT-96M		5.02 $\pm$ 0.04	60M
BTD-96M [44]		9.12	60M
TRACT-256M	2	<b>3.32</b> $\pm$ 0.02	60M
TRACT-96M		3.53 $\pm$ 0.03	60M
TRACT-EDM-256M*		3.55 $\pm$ 0.01	56M
TRACT-EDM-96M*		3.75 $\pm$ 0.02	56M
BTD-96M [44]		4.51	60M

Table 1: FID results on CIFAR-10. <sup>†</sup> Diffusion Fourier Neural Operators (DFNO) use a different model architecture for the student network and require generating a synthetic dataset for training. \* TRACT-EDM models use better teachers.

using the Frechet Inception Distance (FID)[14], computed from 50,000 generated samples. We run each experiment with three seeds to compute the mean and standard deviation. 1-step TRACT models improve FID from 9.1 to 4.5 on CIFAR-10 and from 17.5 to 7.4 on 64x64 ImageNet compared to their BTD [44] counterparts, using the exact same architecture and teacher models. We also present results with TRACT when distilling EDM teacher models [24] using a RK sampler and VE noise schedule: they further improve our FID results to 3.8 on CIFAR-10, see Table (1).

We follow up with ablations of the key components of our method: momentums for self-teaching and inference EMAs, and distillation schedules.

#### 4.1 Image generation results with BTD teachers

The teacher model in each TRACT distillation experiment is initialized from teacher checkpoints of the BTD paper [44]<sup>2</sup> so as to be directly comparable to them.

We use a two-phase  $T : 1024 \rightarrow 32 \rightarrow 1$  distillation schedule. At the start of each phase, the student’s weights are initialized from the current teacher being distilled. In the first phase, the teacher model uses a 1024-step sampling schedule and the student learns to generate samples in 32 steps. In the second phase, the teacher is initialized as the student from the previous phase, and the student learns to generate images in a single step.

**CIFAR-10** We experimented with two training lengths: 96M samples to match the BTD [44] paper, and 256M samples to showcase the benefits of longer training with TRACT. Our 1-step TRACT-96M model obtains an FID of 5.02 that cuts in almost half the previous state-of-the-art of 9.12 [44] with the same architecture and training budget. TRACT-256M further improves our 1-step FID results to 4.45. For both training budgets, we also run distillation experiments ending with a larger number of steps:  $T : 1024 \rightarrow 32 \rightarrow K$  with  $K \in \{2, 4, 8\}$  and obtain state-of-the-art models at all steps. 1 and 2 step results are presented on Table 1 while 4 and 8 step results are presented on Table 7. More experimental details can be found in Appendix A.3.

**64x64 ImageNet** On class-conditional 64x64 ImageNet, our single-step TRACT-96M student achieves a FID of 7.43, which improves our BTD counterpart by 2.4x. Due to resource constraints, we did not distill a TRACT model with as many training samples (1.2B) as BTD [44]. Therefore, the new state-of-the-art that we set on the same model architecture is obtained with a tenth of the training budget. 1 and 2 step results are presented in Table 2 while 4 and 8 step results are presented on Table 8. More experimental details can be found in Appendix A.3.

<sup>2</sup>[https://github.com/google-research/google-research/tree/master/diffusion\\_distillation](https://github.com/google-research/google-research/tree/master/diffusion_distillation)

Method	NFEs	FID	Parameters
TRACT-96M	1	<b>7.43</b> $\pm$ 0.07	296M
TRACT-EDM-96M*		7.52 $\pm$ 0.05	296M
DFNO [51] <sup>†</sup>		8.35	329M
BTD-1.2B [44]		17.5	296M
TRACT-EDM-96M*	2	<b>4.97</b> $\pm$ 0.03	296M
TRACT-96M		5.24 $\pm$ 0.02	296M
BTD-1.2B [44]		7.2	296M

Table 2: FID results on 64x64 ImageNet. <sup>†</sup> Diffusion Fourier Neural Operators (DFNO) use a different model architecture for the student network and require generating a synthetic dataset for training. \* TRACT-EDM models use better teachers.

## 4.2 Image generation results with EDM teachers

EDM models [24] are initialized from checkpoints released with the paper<sup>3</sup>, which are based off NCSN++ architecture[48] for CIFAR-10, and ADM architecture[6] for 64x64 ImageNet. Results for TRACT-EDM models are presented on Table 1 and 7 for CIFAR-10 as well as Table 2 and 8 for 64x64 ImageNet. Experimental details can be found in Appendix A.4.

## 4.3 Stochastic Weight Averaging ablations

TRACT uses two different EMAs: one for the self-teacher and one for the student model used at inference time. The self-teacher uses a fast-moving (low momentum) EMA with momentum  $\mu_S$  and the inference model uses a slow-moving (high momentum) EMA with momentum  $\mu_I$ . We study both momentums across ablations on CIFAR-10.

**Implementation** We use a bias-corrected EMA for our experiments. We detail this implementation for the self-teacher weights  $\tilde{\phi} = \text{EMA}(\phi, \mu_S)$ . At the start of training  $\tilde{\phi}_0 = \phi_0$ , and it is updated at each training step  $i > 0$  with:

$$\tilde{\phi}_i = \left(1 - \frac{1 - \mu_S}{1 - \mu_S^i}\right) \tilde{\phi}_{i-1} + \frac{1 - \mu_S}{1 - \mu_S^i} \phi_i, \quad (16)$$

We use the same implementation for the inference model weights  $\text{EMA}(\phi, \mu_I)$

**Self-teaching EMA** The momentum parameter  $\mu_S$  for the self-teaching EMA strikes a balance between convergence speed and training stability. With low  $\mu_S$ , the self-teacher weights adapt rapidly to training updates but incorporate noise from the optimization process, leading to unstable self-teaching. On the other hand, higher  $\mu_S$  values yield stable self-teaching targets but introduce latency between the student model state and that of its self-teacher. This, in turn, results in outdated self-teacher targets yielding slower convergence.

For the ablation study of  $\mu_S$ , we fixed the distillation schedule to  $T : 1024 \rightarrow 32 \rightarrow 1$ , the training length to 48M samples per phase and  $\mu_I$  to 0.99995. Results are presented in Table 3<sup>4</sup>. Performance decreases monotonically as the self-teaching EMA grows above a certain threshold (about 0.9 in this setting), which supports the slower convergence hypothesis for high values of this parameter. Results are equally worse for values at or below 0.01 and present a high variance. Similarly to observations made in BYOL [11], we found that a wide range of momentum parameter  $\mu_S \in [0.1, 0.9]$  values gives good performance. In light of this, we set  $\mu_S = 0.5$  for all other experiments.

**Inference EMA** We use a slow-moving EMA of student weights at inference time, which has been shown empirically to yield better test time performance [21]. For the ablation study of  $\mu_I$ , we fix the distillation schedule to  $T : 1024 \rightarrow 32 \rightarrow 1$ , training length per phase to 48M samples and  $\mu_S = 0.5$ . Results are presented in Table 4, we observe that values of  $\mu_I$  strongly affect performance. In A.7

<sup>3</sup><https://nvlabs-fi-cdn.nvidia.com/edm/pretrained/>

<sup>4</sup>The best result in the table does not match our best: throughout ablations, for simplicity and at the cost of performance, we did not allocate a larger share of the training budget to the  $32 \rightarrow 1$  distillation phase

Self-teaching EMA	1 step FID	Inference EMA	1 step FID
0.0	6.32		
0.001	6.38		
0.01	7.29	0.999	6.91
0.1	5.34	0.9999	5.5
0.5	<b>5.24</b>	0.99995	<b>5.24</b>
0.9	6.04	0.99999	8.73
0.99	7.61		
0.999	8.30		

Table 3: Self-teaching EMA ablation results on CIFAR-10.

Table 4: Inference time EMA ablation results on CIFAR-10.

we share a heuristic to compute  $\mu_I$  values yielding high quality results across experiments and for varying training lengths.

#### 4.4 Influence of the number of distillation phases

In the VP setting, we find that TRACT performs best when using a 2-phase  $T : 1024 \rightarrow 32 \rightarrow 1$  distillation schedule. Confirming our original conjecture, we observe that schedules with more phases suffer more from *objective degeneracy*. However, we observe the worst results were obtained with a single-phase distillation  $T : 1024 \rightarrow 1$ . In that case, we suspect that due to the long chain of time steps, a phenomenon similar to gradient vanishing is happening. We present ablation results on CIFAR-10 with distillation schedules of increasing number of phases from 1 to 5:  $T : 1024 \rightarrow 1$ ,  $T : 1024 \rightarrow 32 \rightarrow 1$ ,  $T : 4096 \rightarrow 256 \rightarrow 16 \rightarrow 1$ ,  $T : 4096 \rightarrow 512 \rightarrow 64 \rightarrow 8 \rightarrow 1$ ,  $T : 1025 \rightarrow 256 \rightarrow 64 \rightarrow 16 \rightarrow 4 \rightarrow 1$ .

**Fixed overall training length** We set  $\mu_I = 0.99995$ ,  $\mu_S = 0.5$  and the overall training length to 96M samples. Single-step FID results are presented in Table 5. Results clearly get worse with more distillation phases, providing support to the objective degeneracy hypothesis.

Distillation schedule	Phases	Training length	1 step FID
1024, 1	1	96M	14.40
1024, 32, 1	2	96M	<b>5.24</b>
4096, 256, 16, 1	3	96M	6.06
4096, 512, 64, 8, 1	4	96M	7.27
1024, 256, 64, 16, 4, 1	5	96M	8.33

Table 5: Time Schedule ablations with fixed overall training length on CIFAR-10.

**Fixed training length per phase** TRACT with 3, 4 and 5 phase distillation schedules is trained again with an increased training budget, now set to 48M samples *per phase*. 1-step FID results are presented in Table 6. Many-phase schedules improve their performance but FID scores are still worse than with the 2-phase schedule, despite leveraging the same training budget per distillation phase. This suggests that the objective degeneracy problem cannot be fully solved at the cost of a reasonably higher training budget. Meanwhile, as seen in previous experiments (see Table (1)), 2-phase results with 256M samples improved markedly over 96M samples. Therefore, with a fixed training budget, distilling a 2-phase TRACT for longer might be the best choice.

Distillation schedule	Phases	Training length	FID
1024, 32, 1	2	96M	<b>5.24</b>
4096, 256, 16, 1	3	144M	5.76
4096, 512, 64, 8, 1	4	192M	6.83
1024, 256, 64, 16, 4, 1	5	240M	7.04

Table 6: Time Schedule ablations with fixed training length per phase on CIFAR-10.



**Binary Distillation comparison** To further confirm that objective degeneracy is the reason why TRACT outperforms BTM [44], we compare BTM to TRACT on the same BTM-compatible schedule: the 10 phases  $T : 1024 \rightarrow 512 \rightarrow 256 \rightarrow \dots \rightarrow 2 \rightarrow 1$ . We set  $\mu_I = 0.99995$  and 48M training samples per distillation phase for both experiments. In this setting, BTM outperforms TRACT with an FID of 5.95 versus 6.8. This is additional confirmation that BTM’s inferior overall performance may come from its inability to leverage 2-phase distillation schedules. Besides the schedule, the other difference between the BTM and TRACT is the use of self-teaching by TRACT. This experiment also suggests that self-teaching may result in less efficient objectives than supervised training.

#### 4.5 Beyond time distillation

In addition to reducing quality degradation with fewer sampling steps, TRACT can be used for knowledge distillation to other architectures, in particular smaller ones. Compared to TRACT-96M, we show a degradation from 5.02 to 6.47 FID at 1 sampling step on CIFAR-10 by distilling a model from 60.0M parameters to 19.4M. For more details, refer to A.9.

## 5 Conclusion

Generating samples in a single step can greatly improve the tractability of diffusion models. We introduce TRANSITIVE Closure Time-distillation (TRACT), a new method that significantly improves the quality of generated samples from a diffusion model in a few steps. This result is achieved by distilling a model in fewer phases and with stronger stochastic weight averaging than prior methods. Experimentally, we show that without architecture changes to prior work, TRACT improves single-step FID by up to  $2.4\times$ . Further experiments demonstrate that TRACT can also effectively distill to other architectures, in particular to smaller student architectures. While demonstrated on images datasets, our method is general and makes no particular assumption about the type of data. It is left to future work to apply it to other types of data.

An interesting extension of TRACT could further improve the quality-efficiency trade-off: typically, distillation steps in DDIMs/DDPMs have maxed out at 8192 due to computational costs of sampling. Since TRACT allows arbitrary reductions in steps between training phases, we could feasibly distill from much higher step counts teachers, where prior methods could not. This unexplored avenue could open new research into difficult tasks where diffusion models could not previously be applied.

#### Acknowledgements

We would like to thank Josh Susskind, Xiaoying Pang, Miguel Angel Bautista Martin and Russ Webb for their feedback and suggestions.

#### Contributions

Here are the authors contributions to the work: David Berthelot led the research and came up with the transitive closure method and working code prototypes. Arnaud Autef obtained CIFAR-10 results, designed and ran ablation experiments, set up multi-gpu and multi-node training via DDP. Walter Talbott helped with ablation experiments and with writing. Daniel Zheng worked on cloud compute infrastructure, set up multi-gpu and multi-node training via DDP, and ran experiments. Siyuan Hu implemented the FID, integrated the BTM paper’s model into transitive closure framework and conducted the experiments of distillation to smaller architectures. Jierui Lin finalized data, training and evaluation pipeline, obtained 64x64 ImageNet results, integrated BTM’s teacher models and noise schedule to our pipeline, reproduced binary distillation and its variants for ablation. Dian Ang Yap implemented EDM variants, and designed experiments for TRACT (VE-EDM) on CIFAR-10 and ImageNet. Shuangfei Zhai contributed to the discussions, writing and ablation studies. Eric Gu contributed to writing and conducted experiments for distillation to smaller architectures.

## References

- [1] Uri M Ascher and Linda R Petzold. *Computer methods for ordinary differential equations and differential-algebraic equations*, volume 61. Siam, 1998.

- [2] Jacob Austin, Daniel D Johnson, Jonathan Ho, Daniel Tarlow, and Rianne van den Berg. Structured denoising diffusion models in discrete state-spaces. *Advances in Neural Information Processing Systems*, 34:17981–17993, 2021.
- [3] Mark Chen, Alec Radford, Rewon Child, Jeffrey Wu, Heewoo Jun, David Luan, and Ilya Sutskever. Generative pretraining from pixels. In *International conference on machine learning*, pages 1691–1703. PMLR, 2020.
- [4] Nanxin Chen, Yu Zhang, Heiga Zen, Ron J Weiss, Mohammad Norouzi, and William Chan. Wavegrad: Estimating gradients for waveform generation. *arXiv preprint arXiv:2009.00713*, 2020.
- [5] Ricky TQ Chen, Yulia Rubanova, Jesse Bettencourt, and David K Duvenaud. Neural ordinary differential equations. *Advances in neural information processing systems*, 31, 2018.
- [6] Prafulla Dhariwal and Alexander Nichol. Diffusion models beat gans on image synthesis. *Advances in Neural Information Processing Systems*, 34:8780–8794, 2021.
- [7] Laurent Dinh, Jascha Sohl-Dickstein, and Samy Bengio. Density estimation using real NVP. In *International Conference on Learning Representations*, 2017. URL <https://openreview.net/forum?id=HkpbhH91x>.
- [8] John R Dormand and Peter J Prince. A family of embedded runge-kutta formulae. *Journal of computational and applied mathematics*, 6(1):19–26, 1980.
- [9] Shansan Gong, Mukai Li, Jiangtao Feng, Zhiyong Wu, and LingPeng Kong. Diffuseq: Sequence to sequence text generation with diffusion models. *arXiv preprint arXiv:2210.08933*, 2022.
- [10] Ian Goodfellow, Jean Pouget-Abadie, Mehdi Mirza, Bing Xu, David Warde-Farley, Sherjil Ozair, Aaron Courville, and Yoshua Bengio. Generative adversarial networks. *Communications of the ACM*, 63(11):139–144, 2020.
- [11] Jean-Bastien Grill, Florian Strub, Florent Alché, Corentin Tallec, Pierre Richemond, Elena Buchatskaya, Carl Doersch, Bernardo Avila Pires, Zhaohan Guo, Mohammad Gheshlaghi Azar, et al. Bootstrap your own latent-a new approach to self-supervised learning. *Advances in neural information processing systems*, 33:21271–21284, 2020.
- [12] Jiatao Gu, Shuangfei Zhai, Yizhe Zhang, Miguel Ángel Bautista, and Joshua M. Susskind. f-DM: A multi-stage diffusion model via progressive signal transformation. In *International Conference on Learning Representations*, 2023. URL <https://openreview.net/forum?id=iBdwKIsg4m>.
- [13] Seungu Han and Junhyeok Lee. Nu-wave 2: A general neural audio upsampling model for various sampling rates. *arXiv preprint arXiv:2206.08545*, 2022.
- [14] Martin Heusel, Hubert Ramsauer, Thomas Unterthiner, Bernhard Nessler, Günter Klambauer, and Sepp Hochreiter. Gans trained by a two time-scale update rule converge to a nash equilibrium. *CoRR*, abs/1706.08500, 2017. URL <http://arxiv.org/abs/1706.08500>.
- [15] Jonathan Ho, Ajay Jain, and Pieter Abbeel. Denoising diffusion probabilistic models. *Advances in Neural Information Processing Systems*, 33:6840–6851, 2020.
- [16] Jonathan Ho, Chitwan Saharia, William Chan, David J Fleet, Mohammad Norouzi, and Tim Salimans. Cascaded diffusion models for high fidelity image generation. *J. Mach. Learn. Res.*, 23(47):1–33, 2022.
- [17] Marlis Hochbruck and Alexander Ostermann. Explicit exponential runge–kutta methods for semilinear parabolic problems. *SIAM Journal on Numerical Analysis*, 43(3):1069–1090, 2005.
- [18] Marlis Hochbruck and Alexander Ostermann. Exponential integrators. *Acta Numerica*, 19: 209–286, 2010.
- [19] Emiel Hoogeboom, Didrik Nielsen, Priyank Jaini, Patrick Forré, and Max Welling. Argmax flows and multinomial diffusion: Learning categorical distributions. *Advances in Neural Information Processing Systems*, 34:12454–12465, 2021.

- [20] Rongjie Huang, Zhou Zhao, Huadai Liu, Jinglin Liu, Chenye Cui, and Yi Ren. Prodiff: Progressive fast diffusion model for high-quality text-to-speech. In *Proceedings of the 30th ACM International Conference on Multimedia*, pages 2595–2605, 2022.
- [21] Pavel Izmailov, Dmitrii Podoprikin, Timur Garipov, Dmitry P. Vetrov, and Andrew Gordon Wilson. Averaging weights leads to wider optima and better generalization. In Izmailov et al. [21], pages 876–885. URL <http://dblp.uni-trier.de/db/conf/uai/uai2018.html#IzmailovPGVW18>.
- [22] Myeonghun Jeong, Hyeongju Kim, Sung Jun Cheon, Byoung Jin Choi, and Nam Soo Kim. Diff-tts: A denoising diffusion model for text-to-speech. *arXiv preprint arXiv:2104.01409*, 2021.
- [23] Alexia Jolicoeur-Martineau, Ke Li, Rémi Piché-Taillefer, Tal Kachman, and Ioannis Mitliagkas. Gotta go fast when generating data with score-based models. *arXiv preprint arXiv:2105.14080*, 2021.
- [24] Tero Karras, Miika Aittala, Timo Aila, and Samuli Laine. Elucidating the design space of diffusion-based generative models. In Alice H. Oh, Alekh Agarwal, Danielle Belgrave, and Kyunghyun Cho, editors, *Advances in Neural Information Processing Systems*, 2022. URL <https://openreview.net/forum?id=k7FuTOWM0c7>.
- [25] Zhifeng Kong, Wei Ping, Jiaji Huang, Kexin Zhao, and Bryan Catanzaro. Diffwave: A versatile diffusion model for audio synthesis. *arXiv preprint arXiv:2009.09761*, 2020.
- [26] Dong-Hyun Lee et al. Pseudo-label: The simple and efficient semi-supervised learning method for deep neural networks. In *Workshop on challenges in representation learning, ICML*, volume 3, page 896, 2013.
- [27] Junhyeok Lee and Seungu Han. Nu-wave: A diffusion probabilistic model for neural audio upsampling. *arXiv preprint arXiv:2104.02321*, 2021.
- [28] Haoying Li, Yifan Yang, Meng Chang, Shiqi Chen, Huajun Feng, Zhihai Xu, Qi Li, and Yueting Chen. Srdiff: Single image super-resolution with diffusion probabilistic models. *Neurocomputing*, 479:47–59, 2022.
- [29] Xiang Lisa Li, John Thickstun, Ishaan Gulrajani, Percy Liang, and Tatsunori B Hashimoto. Diffusion-lm improves controllable text generation. *arXiv preprint arXiv:2205.14217*, 2022.
- [30] Timothy P. Lillicrap, Jonathan J. Hunt, Alexander Pritzel, Nicolas Heess, Tom Erez, Yuval Tassa, David Silver, and Daan Wierstra. Continuous control with deep reinforcement learning. In Yoshua Bengio and Yann LeCun, editors, *4th International Conference on Learning Representations, ICLR 2016, San Juan, Puerto Rico, May 2-4, 2016, Conference Track Proceedings*, 2016. URL <http://arxiv.org/abs/1509.02971>.
- [31] Jinglin Liu, Chengxi Li, Yi Ren, Feiyang Chen, Peng Liu, and Zhou Zhao. Diffsinger: Diffusion acoustic model for singing voice synthesis. *arXiv preprint arXiv:2105.02446*, 2021.
- [32] Cheng Lu, Yuhao Zhou, Fan Bao, Jianfei Chen, Chongxuan Li, and Jun Zhu. Dpm-solver: A fast ode solver for diffusion probabilistic model sampling in around 10 steps. *arXiv preprint arXiv:2206.00927*, 2022.
- [33] Eric Luhman and Troy Luhman. Knowledge distillation in iterative generative models for improved sampling speed. *arXiv preprint arXiv:2101.02388*, 2021.
- [34] Chenlin Meng, Ruiqi Gao, Diederik P Kingma, Stefano Ermon, Jonathan Ho, and Tim Salimans. On distillation of guided diffusion models. *arXiv preprint arXiv:2210.03142*, 2022.
- [35] Gautam Mittal, Jesse Engel, Curtis Hawthorne, and Ian Simon. Symbolic music generation with diffusion models. *arXiv preprint arXiv:2103.16091*, 2021.
- [36] Takuma Okamoto, Tomoki Toda, Yoshinori Shiga, and Hisashi Kawai. Noise level limited sub-modeling for diffusion probabilistic vocoders. In *ICASSP 2021-2021 IEEE International Conference on Acoustics, Speech and Signal Processing (ICASSP)*, pages 6029–6033. IEEE, 2021.

- [37] Adam Paszke, Sam Gross, Francisco Massa, Adam Lerer, James Bradbury, Gregory Chanan, Trevor Killeen, Zeming Lin, Natalia Gimelshein, Luca Antiga, Alban Desmaison, Andreas Kopf, Edward Yang, Zachary DeVito, Martin Raison, Alykhan Tejani, Sasank Chilamkurthy, Benoit Steiner, Lu Fang, Junjie Bai, and Soumith Chintala. Pytorch: An imperative style, high-performance deep learning library. In *Advances in Neural Information Processing Systems 32*, pages 8024–8035. Curran Associates, Inc., 2019. URL <http://papers.neurips.cc/paper/9015-pytorch-an-imperative-style-high-performance-deep-learning-library.pdf>.
- [38] William Peebles and Saining Xie. Scalable diffusion models with transformers. *arXiv preprint arXiv:2212.09748*, 2022.
- [39] Vadim Popov, Ivan Vovk, Vladimir Gogoryan, Tasnima Sadekova, and Mikhail Kudinov. Grad-tts: A diffusion probabilistic model for text-to-speech. In *International Conference on Machine Learning*, pages 8599–8608. PMLR, 2021.
- [40] Aditya Ramesh, Prafulla Dhariwal, Alex Nichol, Casey Chu, and Mark Chen. Hierarchical text-conditional image generation with clip latents. *arXiv preprint arXiv:2204.06125*, 2022.
- [41] Robin Rombach, Andreas Blattmann, Dominik Lorenz, Patrick Esser, and Björn Ommer. High-resolution image synthesis with latent diffusion models. In *Proceedings of the IEEE/CVF Conference on Computer Vision and Pattern Recognition*, pages 10684–10695, 2022.
- [42] Chitwan Saharia, William Chan, Saurabh Saxena, Lala Li, Jay Whang, Emily Denton, Seyed Kamyar Seyed Ghasemipour, Raphael Gontijo-Lopes, Burcu Karagol Ayan, Tim Salimans, Jonathan Ho, David J. Fleet, and Mohammad Norouzi. Photorealistic text-to-image diffusion models with deep language understanding. In Alice H. Oh, Alekh Agarwal, Danielle Belgrave, and Kyunghyun Cho, editors, *Advances in Neural Information Processing Systems*, 2022. URL <https://openreview.net/forum?id=08Yk-n512A1>.
- [43] Chitwan Saharia, Jonathan Ho, William Chan, Tim Salimans, David J Fleet, and Mohammad Norouzi. Image super-resolution via iterative refinement. *IEEE Transactions on Pattern Analysis and Machine Intelligence*, 2022.
- [44] Tim Salimans and Jonathan Ho. Progressive distillation for fast sampling of diffusion models. In *International Conference on Learning Representations*, 2022. URL <https://openreview.net/forum?id=TIIdIXIpzhoI>.
- [45] Jascha Sohl-Dickstein, Eric Weiss, Niru Maheswaranathan, and Surya Ganguli. Deep unsupervised learning using nonequilibrium thermodynamics. In *International Conference on Machine Learning*, pages 2256–2265. PMLR, 2015.
- [46] Jiaming Song, Chenlin Meng, and Stefano Ermon. Denoising diffusion implicit models. *arXiv preprint arXiv:2010.02502*, 2020.
- [47] Yang Song and Stefano Ermon. Generative modeling by estimating gradients of the data distribution. *Advances in neural information processing systems*, 32, 2019.
- [48] Yang Song, Jascha Sohl-Dickstein, Diederik P Kingma, Abhishek Kumar, Stefano Ermon, and Ben Poole. Score-based generative modeling through stochastic differential equations. In *International Conference on Learning Representations*, 2021. URL <https://openreview.net/forum?id=PxtTIG12RRHS>.
- [49] Endre Süli and David F Mayers. *An introduction to numerical analysis*. Cambridge university press, 2003.
- [50] Arash Vahdat, Karsten Kreis, and Jan Kautz. Score-based generative modeling in latent space. *Advances in Neural Information Processing Systems*, 34:11287–11302, 2021.
- [51] Hongkai Zheng, Weili Nie, Arash Vahdat, Kamyar Azizzadenesheli, and Anima Anandkumar. Fast sampling of diffusion models via operator learning. *arXiv preprint arXiv:2211.13449*, 2022.

## A Appendix

### A.1 Deriving the distillation target $\hat{x}$

We want our student network to match the closure of the teacher steps via self-teaching. If the student network is perfect we have:

$$\delta(g_\phi, x_t, t, t_i) = \delta(g_{\tilde{\phi}}, \delta(f_\theta, x_t, t, t-1), t-1, t_i)$$

We write the right-hand term  $x_{t_i} := \delta(g_{\tilde{\phi}}, \delta(f_\theta, x_t, t, t-1), t-1, t_i)$  and develop equations for the training target to obtain a perfect student:

$$\begin{aligned} x_{t_i} &= \delta(g_\phi, x_t, t, t_i) \\ x_{t_i} &= \sqrt{\gamma_{t_i}} g_\phi(x_t, t) + \sqrt{1-\gamma_{t_i}} \left( \frac{x_t - \sqrt{\gamma_t} g_\phi(x_t, t)}{\sqrt{1-\gamma_t}} \right) \\ x_{t_i} &= \left( \sqrt{\gamma_{t_i}} - \frac{\sqrt{\gamma_t} \sqrt{1-\gamma_{t_i}}}{\sqrt{1-\gamma_t}} \right) g_\phi(x_t, t) + \frac{\sqrt{1-\gamma_{t_i}}}{\sqrt{1-\gamma_t}} x_t \\ x_{t_i} \sqrt{1-\gamma_t} &= \left( \sqrt{\gamma_{t_i}} \sqrt{1-\gamma_t} - \sqrt{\gamma_t} \sqrt{1-\gamma_{t_i}} \right) g_\phi(x_t, t) + \sqrt{1-\gamma_{t_i}} x_t \\ g_\phi(x_t, t) &= \frac{x_{t_i} \sqrt{1-\gamma_t} - x_t \sqrt{1-\gamma_{t_i}}}{\sqrt{\gamma_{t_i}} \sqrt{1-\gamma_t} - \sqrt{\gamma_t} \sqrt{1-\gamma_{t_i}}} \end{aligned}$$

### A.2 Deriving the distillation loss

The signal training loss is derived from the noise training loss between the expected noise  $\epsilon$  and predicted noise  $\epsilon_{|t}$  as follows:

$$\begin{aligned} \mathcal{L}(\phi) &= \|\epsilon_{|t} - \epsilon\|_2^2 \\ &= \left\| \frac{x_t - g_\phi(x_t, t) \sqrt{\gamma_t}}{\sqrt{1-\gamma_t}} - \frac{x_t - \hat{x} \sqrt{\gamma_t}}{\sqrt{1-\gamma_t}} \right\|_2^2 \\ &= \frac{\gamma_t}{1-\gamma_t} \|g_\phi(x_t, t) - \hat{x}\|_2^2 \end{aligned}$$

In code implementation, it is common for numerical reasons to use:

$$\mathcal{L}(\phi) = \max \left( 1, \frac{\gamma_t}{1-\gamma_t} \right) \|g_\phi(x_t, t) - \hat{x}\|_2^2$$

### A.3 Experimental details for TRACT

**CIFAR-10** To obtain our best performing TRACT-96M and TRACT-256M, we use a global batch size of 256 split across 8 GPUs and the Adam optimizer with a constant learning rate of  $2 \times 10^{-4}$ , no weight decay, no dropout, and gradient clipping to a norm of 1.0.

The momentum parameter of the self-teaching EMA  $\tilde{\phi}$  is set to  $\mu_S = 0.5$  during distillation. At sampling time, we use another EMA of the student weights to generate images, whose momentum parameter  $\mu_I$  is set to a higher value: 0.99997 for TRACT-96M and 0.99999 for TRACT-256M. Finally, like in [44] we allocate higher distillation budgets to the  $32 \rightarrow 1$  than to the  $1024 \rightarrow 32$  phase. We suspect that the optimal balance between the two stages depends on the overall training length, but did not overly tune this hyperparameter and split total training samples  $1/6$  for phase  $1024 \rightarrow 32$  and  $5/6$  for phase  $32 \rightarrow 1$  in both experiments.

Method	NFEs	FID	Parameters
TRACT-256M	4	<b>2.93</b> $\pm$ 0.04	60M
BTD-96M [44]		3.00	60M
TRACT-96M		3.16 $\pm$ 0.14	60M
TRACT-EDM-256M*		3.21 $\pm$ 0.01	56M
TRACT-EDM-96M*		3.41 $\pm$ 0.02	56M
TRACT-EDM-256M*	8	<b>2.41</b> $\pm$ 0.01	56M
TRACT-EDM-96M*		2.48 $\pm$ 0.01	56M
BTD-96M [44]		2.57	60M
TRACT-96M		2.80 $\pm$ 0.05	60M
TRACT-256M		2.84 $\pm$ 0.01	60M

Table 7: FID results on CIFAR-10. † Diffusion Fourier Neural Operators use a different model architecture for the student network and require generating a synthetic dataset for training. \* TRACT-EDM models use better teachers.

**64x64 ImageNet** We use a global batch size of 256 split across 8 GPUs for our best performing TRACT-96M. We use Adam optimizer with a constant learning rate of  $2 \times 10^{-4}$ , no weight decay, no dropout, and gradient clipping to a norm of 1.0.

The momentum parameter of the self-teaching EMA  $\tilde{\phi}$  is set to  $\mu_S = 0.5$  during distillation. At sampling time, we use another EMA of the student weights to generate images, whose momentum parameter  $\mu_I$  is set to a higher value of 0.99995 for TRACT-96M. We evenly split the overall training length between phase  $1024 \rightarrow 32$  and phase  $32 \rightarrow 1$ .

Unlike for CIFAR10 experiments, we predict both signal  $x_0$  and noise  $\epsilon_0$  during distillation, following the setup of BTD [44].

#### A.4 Experimental details for TRACT with EDM teachers

**CIFAR-10** We use NCSN++ by Song et. al. [48] and pretrained weights from Karras et. al. [24]. Without augmentation, our model contains 56 million trainable parameters. We use a global batch size of 512 split across 8 GPUs for our best performing TRACT-96M and TRACT-256M. We use Adam optimizer with a constant learning rate of  $1 \times 10^{-3}$  for one-step distillation, and learning rate of  $3 \times 10^{-4}$  for multi-step distillation. For all settings, we disable weight decay, learning rate warmup, dropout, augmentation, and gradient clipping.

As EDM samplers require lower NFEs compared to typical DDIM samplers, we tune the hyperparameter of timesteps to distill from. We find that distilling from 40 steps (79 NFEs with Runge-Kutta) to 1 step gives a good balance between generating high quality targets from teachers, and ease of learning for the student.

**64x64 ImageNet** For class-conditional 64x64 ImageNet, we use ADM model by Dhariwal and Nichol [6] with 296 million parameters and weights from Karras et. al. [24] with no changes. We train the model with a global batch size of 512 split across 8 A100 GPUs, with Adam optimizer of a constant learning rate of  $3 \times 10^{-4}$  with a linear learning rate warm-up of 4M samples. We disable weight decay, dropout, augmentation, and gradient clipping as we do not observe impacts on the final FID scores. As 64x64 ImageNet uses a different model targeted for higher resolutions, we apply a one-phase distillation from 128 timesteps (255 NFEs with Runge-Kutta) to one-step or multi-step for improved targets from the teacher.

#### A.5 More experimental results

In Table 7 and 8, we show the results of distilling to 4-step and 8-step student models on CIFAR10 and 64x64 ImageNet. Performance is slightly worse than BTD [44], possibly due to self-teaching being less efficient than supervised training as discussed in Section 4.4.

Method	NFEs	FID	Parameters
BTD-1.2B [44]	4	<b>3.9</b>	296M
TRACT-96M		$4.32 \pm 0.07$	296M
TRACT-EDM-96M*		$5.25 \pm 0.32$	296M
BTD-1.2B [44]	8	<b>2.9</b>	296M
TRACT-96M		$3.88 \pm 0.05$	296M
TRACT-EDM-96M*		$3.93 \pm 0.06$	296M

Table 8: FID results on 64x64 ImageNet. † Diffusion Fourier Neural Operators use a different model architecture for the student network and require generating a synthetic dataset for training. \* TRACT-EDM models use better teachers.

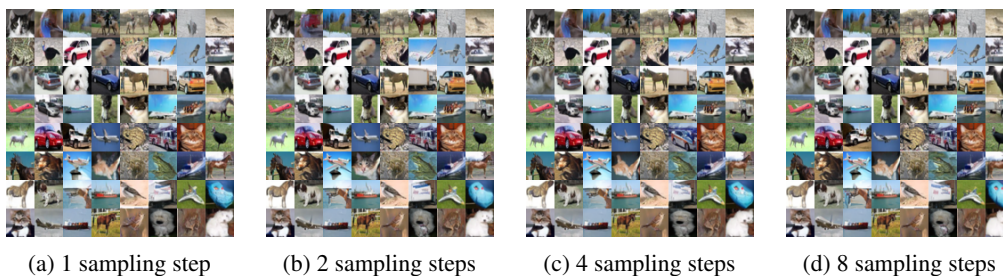


Figure 2: Random samples from TRACT-256M on CIFAR10, for a fixed initial noise with varying number of sampling steps.

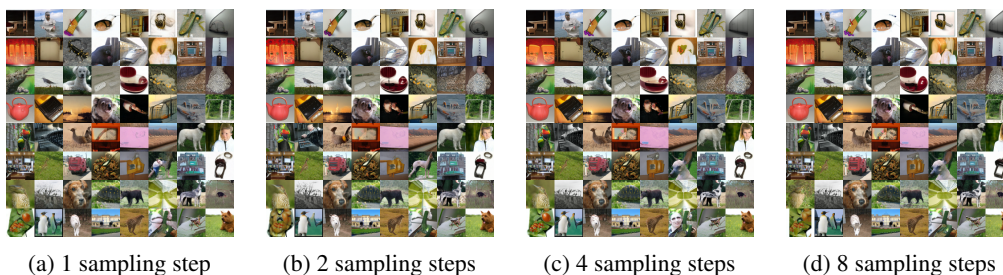


Figure 3: Random samples from TRACT-96M on  $64 \times 64$  ImageNet, for a fixed initial noise and class label with varying number of sampling steps.

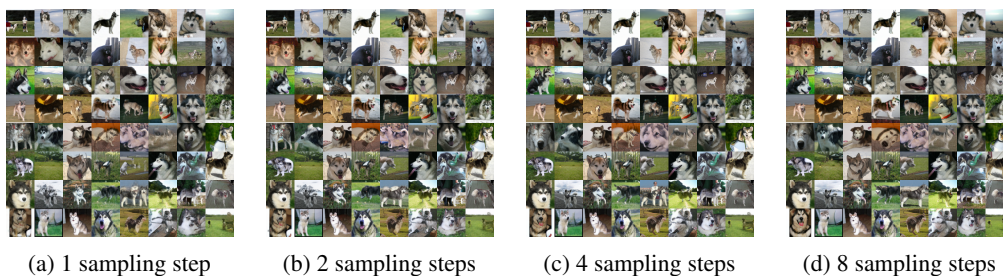


Figure 4: Random samples from TRACT-96M on  $64 \times 64$  ImageNet, conditioned on the 'malamute' class, for a fixed initial noise with varying number of sampling steps.

## A.6 Generated samples

We present random samples from our distilled models with varying sampling steps. As shown in Figure 2, 3 and 4, the deterministic mapping between noises and samples are mostly preserved in these distilled models. We can see that there is a slight degrade of image quality for the 1-step student compared with students distilled to more sampling steps.

## A.7 A heuristic to pick the EMA momentum parameter

In our experiments, we evidenced that  $\mu_I$ , the EMA momentum parameter for our evaluation model, is key to good performance and must be tuned carefully. This motivated us to come up with a heuristic to pick it efficiently.

We hypothesize that this momentum parameter should be as high as possible while keeping the EMA unbiased to model parameter values at initialization: at the end of training, the weight of initial student parameters should be small in the EMA of model parameters. Formally, training a model over  $N$  steps we obtain a sequence of model weights  $(\theta_i)_{0 \leq i \leq N}$ , where  $\theta_0$  represents the model weights at initialization. At the end of training, the resulting EMA of model weights  $\theta_{EMA}$  used for inference is obtained from:

$$\theta_{EMA} = (1 - \mu_I) \sum_{1 \leq i \leq N} \mu_I^{N-i} \theta_i + \mu_I^N \theta_0$$

In that context, we want  $\mu_I^N$  to be small at the end of training and we call  $\epsilon$  this small value:

$$\mu_I^N := \epsilon$$

We parameterize our heuristic this way: when varying our training length,  $N$  changes but we keep  $\epsilon$  fixed to derive an appropriate  $\mu_I$  value used by the inference time EMA. We picked  $\epsilon = 10^{-4}$  in our experiments and obtained good results with it.

We compare this heuristic to a direct grid search for a fixed  $\mu_I$  parameter. We carry out experiments on CIFAR-10 with 5 different  $\epsilon$  values,  $\epsilon \in \{10^{-1}, 10^{-2}, 10^{-3}, 10^{-4}, 10^{-5}\}$ . For each value, we train 1-step  $T : 1024 \rightarrow 32 \rightarrow 1$  TRACT models over varying training lengths. We vary the number of samples  $S \in \{16M, 32M, 48M, 64M\}$  with a fixed batch size of 256, the number of training steps  $N$  therefore varies as  $S/256$ . We compare results to a grid search for  $\mu_I$  with 5 different values,  $\mu_I \in \{1 - 10^{-3}, 1 - 5 \times 10^{-4}, 1 - 10^{-4}, 1 - 5 \times 10^{-5}, 1 - 10^{-5}\}$ . Those values are also fixed across training lengths. Results are summarized in Figure 5. First, we note that training for longer always improves performance. Then, we notice that the  $\epsilon$  heuristic seems more effective at finding a good performing EMA momentum parameter  $\mu_I$  than a direct grid search. All  $\epsilon$  values reach a reasonable performance and the best performance for a given training length is often for one value of  $\epsilon$ , rather than a  $\mu_I$  found from the direct grid search.

## A.8 TRACT with EDM teachers

In this section, we expand derivations of the TRACT distillation algorithm with EDM [24] teacher models. We keep their VE noise schedule, an RK sampler with the teacher model, and distill them into a DDIM student network.

**DDIM step with VE noise schedule** With a VE noise schedule, starting from a noisy image  $x_t$ ,  $t > 0$  with a signal predicting network  $f_\theta$  we obtain estimates for the signal and the noise as:

$$x_{0|t} := f_\theta(x_t, t) \text{ and } \epsilon_{|t} = \frac{x_t - x_{0|t}}{\sigma_t}$$

The corresponding DDIM step from  $t$  to any  $t'$  is therefore:

$$\begin{aligned} x_{t'} &= x_{0|t} + \sigma_{t'} \epsilon_{|t} \\ x_{t'} &= f_\theta(x_t, t) + \sigma_{t'} \frac{x_t - x_{0|t}}{\sigma_t} \\ \delta_{DDIM-VE}(f_\theta, x_t, t, t') &= x_{t'} = f_\theta(x_t, t) \left(1 - \frac{\sigma_{t'}}{\sigma_t}\right) + \frac{\sigma_{t'}}{\sigma_t} x_t \end{aligned}$$



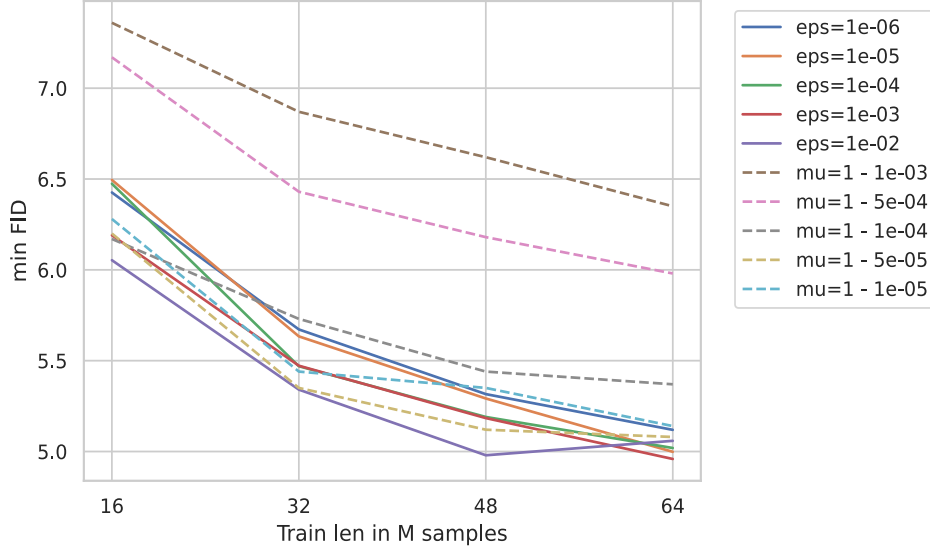


Figure 5: 1-step FID for 2-phases  $T : 1024 \rightarrow 32 \rightarrow 1$  TRACT distilled models. Each curve maps to a different way to set the inference time EMA momentum  $\mu$  across training lengths. Dashed lines correspond to fixing a  $\mu$  value, solid lines correspond to fixing  $\epsilon = \mu^N$ .

**RK sampling** The ODE defined by the VE noise process 10 can be solved by numerical integration from step  $t$  to step  $t' < t$  with a RK solver following the below steps, which define  $\delta_{RK}(f_\theta, x_t, t, t')$ .

$$\begin{aligned} \epsilon|_t &= \frac{x_t - f_\theta(x_t, t)}{\sigma_t} \\ x_{t'} &= x_t + (\sigma_{t'} - \sigma_t)\epsilon|_t \\ \epsilon'|_t &= \frac{x_{t'} - f_\theta(x_{t'}, t')}{\sigma_{t'}} \\ x_{t'} &= x_t + (\sigma_{t'} - \sigma_t) \frac{\epsilon|_t + \epsilon'|_t}{2} \end{aligned}$$

Where the last two steps are skipped when  $t' = 0$ .

**Deriving the distillation target  $\hat{x}$**  We want our student network to match the closure of the teacher steps via self-teaching. If the student network is perfect we have:

$$\delta_{DDIM-VE}(g_\phi, x_t, t, t_i) = \delta_{DDIM-VE}(g_{\tilde{\phi}}, \delta_{RK}(f_\theta, x_t, t, t-1), t-1, t_i)$$

We write the right-hand term  $x_{t_i} := \delta_{DDIM-VE}(g_{\tilde{\phi}}, \delta_{RK}(f_\theta, x_t, t, t-1), t-1, t_i)$  and develop equations for the training target to obtain a perfect student:

$$\begin{aligned} x_{t_i} &= \delta_{DDIM-VE}(g_\phi, x_t, t, t_i) \\ x_{t_i} &= g_\phi(x_t, t) \left(1 - \frac{\sigma_{t_i}}{\sigma_t}\right) + \frac{\sigma_{t_i}}{\sigma_t} x_t \\ x_{t_i} \sigma_t &= g_\phi(x_t, t) (\sigma_t - \sigma_{t_i}) + \sigma_{t_i} x_t \\ g_\phi(x_t, t) &= \frac{x_{t_i} \sigma_t - \sigma_{t_i} x_t}{\sigma_t - \sigma_{t_i}} \end{aligned}$$

We now have all the ingredients to write the TRACT distillation algorithm with EDM teachers, which is presented in Algorithm 2.

## A.9 Knowledge Distillation

TRACT can also be used for knowledge distillation from architecture A to another architecture B using only one additional training phase. Of particular interest is the case when the target architecture

---

**Algorithm 2** Single-phase TRACT (VE-EDM) distillation from T timesteps to T/S timesteps for groups of size S.

---

```

1: Inputs Training data  $\mathcal{X}$ , time schedule  $\gamma \in \mathbb{R}^T$ ,  $f_\theta$  is the teacher,  $g_\phi$  is the student being trained
2:  $\phi \leftarrow \theta$ ;  $\tilde{\phi} \leftarrow \theta$  ▷ Initialize self-teacher and student from teacher
3: for batch of training data  $(x^{(b)}; b \in \{1, \dots, B\}) \sim \mathcal{X}$  do
4:    $\mathcal{L}(\phi) \leftarrow 0$ 
5:   for  $b = 1$  to  $B$  do
6:     sample  $\epsilon \sim \mathcal{N}(0, 1)$ 
7:     sample  $s \sim \{0, S, 2S, \dots, T - S\}$  ▷ Sample the group starting position
8:     sample  $p \sim \{1, \dots, S\}$  ▷ Sample the index within the group
9:      $t \leftarrow s + p$  ▷ Timestep to distill
10:     $x_t \leftarrow x^{(b)} + \sigma_t \epsilon$  ▷ Generate noisy sample
11:    # Step 1. Runge-Kutta Target from the teacher
12:     $\epsilon_{|t} \leftarrow (x_t - f_\theta(x_t, t)) / \sigma_t$ 
13:     $x_{t-1} \leftarrow x_t + (\sigma_{t-1} - \sigma_t) \epsilon_{|t}$ 
14:    if  $\sigma_{t-1} \neq 0$  then
15:       $\epsilon'_{|t} \leftarrow (x_{t-1} - f_\theta(x_{t-1}, t-1)) / \sigma_{t-1}$  ▷ RK second-order correction
16:       $x_{t-1} \leftarrow x_t + \frac{1}{2}(\sigma_{t-1} - \sigma_t)(\epsilon_{|t} + \epsilon'_{|t})$ 
17:    end if
18:    # Step 2. Self-teaching step
19:    if  $s = t - 1$  then
20:       $x_s \leftarrow x_{t-1}$ 
21:    else
22:       $x_s \leftarrow g_{\tilde{\phi}}(x_{t-1}, t-1)(1 - \sigma_s / \sigma_{t-1}) + x_{t-1} \sigma_s / \sigma_{t-1}$  ▷ VE DDIM step
23:    end if
24:    # Step 3. Base case of terminal noise indices
25:    if  $t - 1 = 0$  then
26:      target  $\hat{x} \leftarrow f_\theta(x_t, t)$ 
27:    else
28:      target  $\hat{x} \leftarrow (\sigma_t x_s - x_t \sigma_s) / (\sigma_t - \sigma_s)$ 
29:    end if
30:    Loss  $\mathcal{L}(\phi) \leftarrow \mathcal{L}(\phi) + \frac{1}{B} \lambda(\sigma_t) \|g_\phi(x_t, t) - \text{stop\_gradient}(\hat{x})\|_2^2$  ▷ EDM loss
31:  end for
32:  Compute gradients of  $\mathcal{L}(\phi)$  and update parameters  $\phi$ 
33:  Update  $\tilde{\phi} \leftarrow EMA(\phi, \mu_S)$ 
34: end for

```

---

B has lower computational complexity than A. The additional training phase is a standard distillation (i.e. not time-based), where the number of steps is held constant while the teacher and student have different architectures. For instance, a distillation schedule  $T : 1024 \rightarrow 32 \rightarrow 1$  leads to two possibilities  $T : (1024_A \rightarrow 1024_B) \rightarrow 32_B \rightarrow 1_B$  and  $T : 1024_A \rightarrow (32_A \rightarrow 32_B) \rightarrow 1_B$ . In our experiments, we created the architecture B with 67% fewer parameters by keeping the architecture A (from BTM [44] paper), and reducing the number of channels for each layer from 256 to 128. We show comparable performance in Table 9 on CIFAR-10 with 1 sampling step.

Method	Distillation schedule	Parameters	Training Length	FID
BTM	1024, 512, ... , 1	60.0M	96M	9.12
TRACT	1024, 32, 1	60.0M	96M	5.02
TRACT	1024, 1024, 32, 1	19.4M	432M	7.17
TRACT	1024, 32, 32, 1	19.4M	336M	6.47

Table 9: Single step FID on CIFAR-10.

It could be interesting to validate in future work whether TRACT works with heterogeneous types of model architectures for students and teachers, such as Transformers [38].